Current Transformers and Coupling-Capacitor Voltage Transformers in Real-Time Simulations

J.R.Martí L.R.Linares H.W.Dommel

The University of British Columbia, Vancouver, B.C., Canada

Abstract.— This paper describes two models: a saturable current transformer model (CT) and a wide-band coupling capacitor voltage transformer suitable for real-time transients simulation. By using very efficient network reduction and network synthesis techniques, the operations count for these models is kept to a minimum. The accuracy of the models has been tested in connection with our real-time transients simulator RTNS [1] and compared to conventional EMTP models [2].

Keywords: Current transformers, coupling capacitor voltage transformers, EMT modelling, real-time simulation.

1. Introduction

Under *normal* transient conditions, instrument transformers do not affect the behaviour of the electric power system. It is then possible to model instrument transformers in separate DSP boards, which receive their input from the real-time simulator, and which send their output through amplifiers to protective relays or to other equipment being tested. With the solution being performed in a separate DSP board for each instrument transformer, fast solution algorithms may not be quite as critical as for the real-time simulator itself. Nonetheless, solutions must still be reasonably fast.

This paper describes fast solution algorithms for current transformers and for coupling-capacitor voltage transformers, assuming they have no effect on the power system.

2. Current Transformer

In general, current transformers do not influence the transient behaviour of the electric power network, except in special and unusual circumstances of ferroresonance. With the exception of such special cases, current transformers can therefore be simulated separately from the electric power system. Its primary current will be known from the network solution.

A fast and non-iterative solution method for obtaining the secondary current from the known primary current is described here.

96 SM 389-7 PWRD A paper recommended and approved by the IEEE Power System Relaying Committee of the IEEE Power Engineering Society for presentation at the 1996 IEEE/PES Summer Meeting, July 28 - August 1, 1996, in Denver, Colorado. Manuscript submitted April 15, 1996; made available for printing May 20, 1996.

a) Equivalent circuit

A reasonably accurate equivalent circuit of the current transformer is shown in Fig. 1 with all quantities referred to

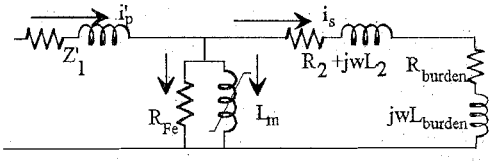

Figure 1. Equivalent circuit of current transformer.

the secondary side, where

i'_p = primary current referred to the secondary side,
i_{Fe} = current through resistance R_{Fe} for the approximation of iron core losses,
i_m = magnetizing current through non-linear inductance,
i_s = secondary current.

Since the primary current i'_p is an impressed current source, the primary leakage impedance Z_1, does not influence the results, and is therefore not needed.

The primary current is the sum of three current components,

$$i'_p = i_{Fe} + i_m + i_s . \tag{1}$$

Each one of the component currents in this equation can be expressed as a function of the flux linkage λ in the transformer core, which leads to a single equation for i_s as a function of i'_p.

b) Core loss branch

The voltage across the core loss resistance is

$$v = R_{Fe} \cdot i_{Fe} , \tag{2}$$

but v is also the voltage in the parallel magnetizing branch,

$$v = \frac{d\lambda}{dt} . \tag{3}$$

With the trapezoidal rule of integration, which is identical to the use of a central difference quotient, and after substituting Eq. (3) into (2), the left-hand side of Eq. (3) becomes $(\lambda_{new} - \lambda_{old})/\Delta t$, and the right-hand side becomes $R_{Fe}(i_{Fe\text{-}new} + i_{Fe\text{-}old})/2$, where subscripts *new* and *old* refer to the values at the present time step t and the preceding time step at $t - \Delta t$, respectively. Therefore,

$$i_{Fe-new} = c_{Fe}\lambda_{new} + h_{Fe-old} , \tag{4a}$$

where the *history term* h_{Fe} contains values from the

0885-8977/97/$10.00 © 1996 IEEE

preceding time step,

$$h_{Fe-old} = -c_{Fe}\lambda_{old} - i_{Fe-old}, \tag{4b}$$

with the constant

$$c_{Fe} = \frac{2}{R_{Fe}\Delta t}. \tag{4c}$$

c) Magnetizing branch

The flux-current relationship of the magnetizing branch is represented by the piecewise linear curve of Fig. 2.

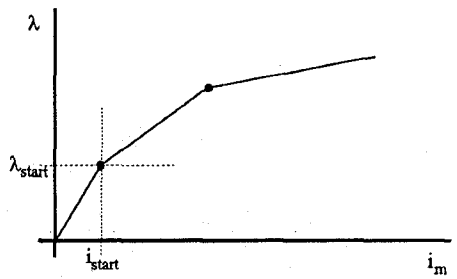

Figure 2. Piecewise linear representation of magnetizing branch.

If the operating point lies in the linear segment starting with $\lambda_{start}/i_{start}$, then

$$i_m - i_{start} = \frac{1}{L}(\lambda - \lambda_{start}), \tag{5}$$

where L is the slope of that segment. This can be rewritten as

$$i_m = \frac{1}{L}\lambda + k_m, \tag{6a}$$

with a known constant k_m for each segment,

$$k_m = i_{start} - \frac{\lambda_{start}}{L}. \tag{6b}$$

d) Secondary side branch

By combining the secondary leakage impedance with the burden into the secondary side impedance

$$R_s + j\omega L_s = (R_2 + R_{burden}) + j(\omega L_2 + \omega L_{burden}), \tag{7}$$

we get

$$v = R_s i_s + L_s \frac{di_s}{dt}, \tag{8a}$$

or with Eq. (3),

$$\frac{\lambda_{new} - \lambda_{old}}{\Delta t} = R_s \frac{i_{s-new} + i_{s-old}}{2} + L_s \frac{i_{s-new} - i_{s-old}}{\Delta t}. \tag{8b}$$

This can be rewritten as

$$i_{s-new} = c_s\lambda_{new} + h_{s-old}, \tag{9a}$$

with the history term

$$h_{s-old} = -c_s\lambda_{old} - d_s i_{s-old}, \tag{9b}$$

and the two constants

$$c_s = \frac{1}{L_s + \frac{R_s\Delta t}{2}}, \quad d_s = c_s\left(\frac{R_s\Delta t}{2} - L_s\right). \tag{9c}$$

e) Secondary current as function of primary current

With Eqs. (1), (4a), (6a) and (9a) we obtain

$$i'_p = i_{Fe} + i_m + i_s = (c_{Fe} + \frac{1}{L} + c_s)\lambda + (h_{Fe} + k_m + h_s). \tag{10}$$

Now let us express λ as a function of i_s with Eq. (9a), and we obtain the desired expression of $i_s = f(i'_p)$ in the form

$$i_s = k_1(i'_p - h_{Fe} - k_m - h_s) + h_s. \tag{11a}$$

where k_1 is the constant

$$k_1 = \frac{c_s}{c_{Fe} + \frac{1}{L} + c_s}. \tag{11b}$$

If the history terms are known from values at the preceding time step, the secondary current can be obtained from the primary current with Eq. (11a) with only one multiplication and four additions.

f) Updating history terms

After the new secondary current $i_{s\text{-new}}$ has been found at time t, the history terms must be updated to advance the solution by Δt.

For the updating calculations, the term $c_s\lambda_{new}$, rather than λ_{new}, is first found from Eq. (9a),

$$c_s\lambda_{new} = i_{s-new} - h_{s-old}. \tag{12}$$

The new history term for the secondary side branch then follows from Eq. (9b),

$$h_{s-new} = -c_s\lambda_{new} - d_s i_{s-new}. \tag{13}$$

The history term for the core loss branch is found from the recursive formula

$$h_{Fe-new} = k_{Fe}(c_s\lambda_{new}) - h_{Fe-old}, \tag{14}$$

which follows from Eq. (4b) if $i_{Fe\text{-new}}$ is replaced with its expression from Eq. (4a). The constant k_{Fe} is

$$k_{Fe} = -\frac{2c_{Fe}}{c_s}. \tag{15}$$

These updating formulas add another 2 multiplications and 3 additions to the effort required in each time step, for a total of 3 multiplications and 7 additions. There is also a check needed to see whether $c_s\lambda_{new}$ in Eq. (13) has taken us into another segment in the piecewise linear representation of the magnetization curve.

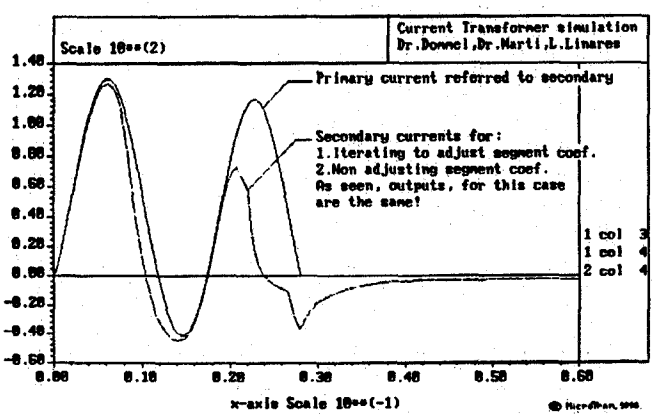

Figure 3.

g) Example

Figure 3 compares the results of this algorithm with the standard EMTP solution method. Both answers are practically identical. This case is taken from a field test comparison described in [3], where six segments were used to represent the magnetization curve. In practice, it is usually possible to use fewer segments and still achieve acceptable accuracy. For the duplication of test results described in [4], simulation results with a two-segment representation were almost as accurate as those from more detailed representations. The *knee point* in a two-segment representation seems to be more important than all other parameters of the saturation curve.

3. Coupling Capacitor Voltage Transformer

A simplified schematic of a coupling capacitor voltage transformer is shown in Fig. 4.

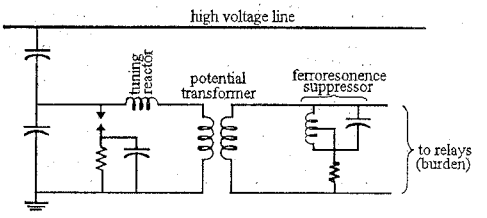

Figure 4. Schematic of a Coupling Capacitor Voltage Transformer.

As reported in [5] and [6], a detailed wide frequency band model of a CCVT is complicated due to the magnetic and capacitive interactions in the various parts of the component magnetic devices (tuning reactor, potential transformer and ferroresonance suppressor).

a) Potential transformer and reactors

Figure 5a shows a lumped-parameter equivalent circuit for a single-phase two-winding transformer [7], 1-3 are the input terminals and 2-4 the output terminals. This representation is valid for frequencies up to the hundreds of kilohertz. The circuit includes the various stray capacitances inside the device: winding to winding (C_{HL}), turn to turn (C_H, C_L) and winding to ground (C_{HG}, C_{LG}), as well as the frequency dependent leakage impedance ($Z_{leak}(\omega)$) and the possibly nonlinear and frequency dependent core magnetization branch $Z_m(\omega)$.

The core magnetization branch is usually more conveniently relocated across the outside terminals of the winding closest to the core (usually the low-voltage winding). This branch can then be modelled by itself with as much detail as desired, or as allowed by the solution time constraints. As noted in [8], the saturation and hysteresis characteristics of this branch can influence the low frequency spectrum of the solution.

For single-coil devices, like the tuning reactor and

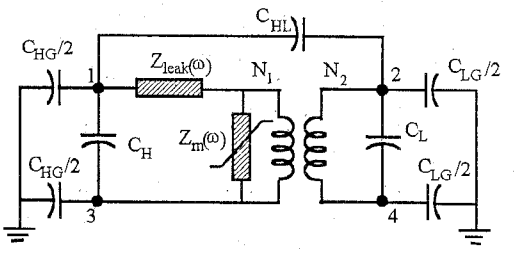

(a) Two-winding transformer.

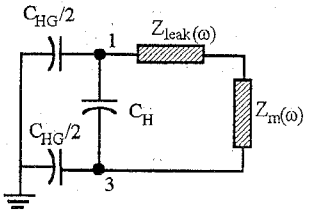

(b) Reactor.

Figure 5. Lumped-parameter high frequency equivalent circuits for two winding transformers and reactors.

ferroresonance suppressor in Fig. 4, the equivalent circuit (Fig. 5b) is *half* the equivalent circuit of the two-winding transformer of Fig 5a. In reactors the *magnetization* branch Z_m is the main impedance of the circuit. Normally, however, reactors are built so as not to saturate and both Z_{leak} and Z_m can be modelled as lineal frequency dependent R-L branches and synthesized in a similar way as $Z_{leak}(\omega)$ in the two winding transformer.

b) Simplified equivalent circuit

Using a circuit transformation [9], the winding to winding capacitance C_{HL}, which bridges both sides of a two-winding transformer, can be moved over to only one side, as indicated in Fig. 6. The result is a capacitance in parallel with Z_{leak} plus additional capacitances in parallel with C_H and C_L.

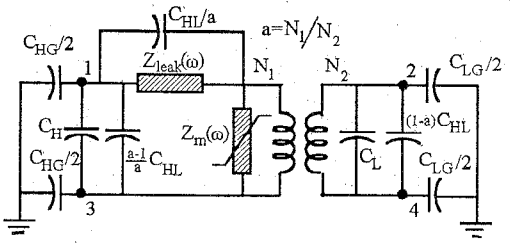

Figure 6. High frequency equivalent circuit for a two-winding transformer.

After subtracting the *outside* capacitances at the terminal ports 1-3 and 2-4, the impedance Z_{leak} in parallel with C_{HL}/a is the short-circuit impedance measured during a short-circuit test. As described in [7], the various capacitances of this

equivalent circuit, as well as the short-circuit impedance Z_{short} (Z_{leak} in parallel with C_{HL}/a) can be obtained directly from simple measurements. A typical measured short-circuit impedance response is shown in Fig. 7.

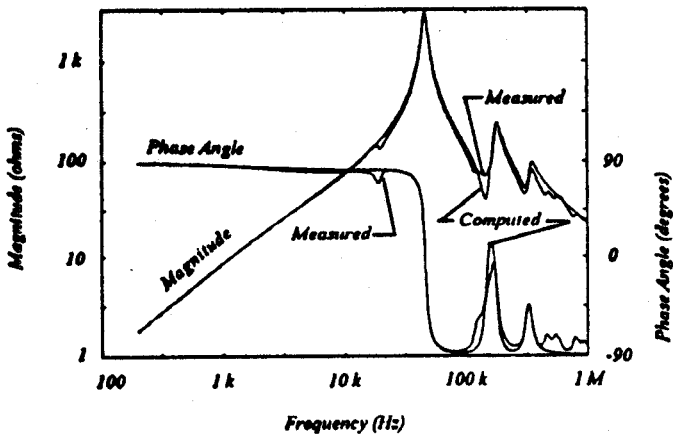

Figure 7. Short-circuit impedance (Z_{short}) of a two-winding transformer: measured and synthesized responses.

It is shown in [7] that $Z_{short}(\omega)$ (Fig. 7) can be matched very accurately using a number of *RLC* blocks: one block per resonant peak (Fig. 8a).

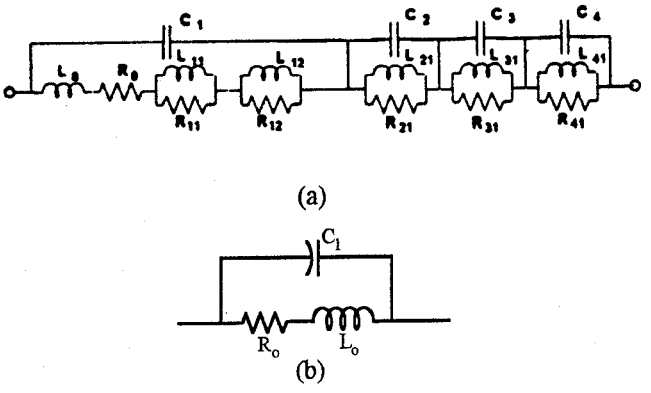

Figure 8. Synthesis *RLC* network to approximate $Z_{short}(\omega)$. (a) Multiple peak high-accuracy synthesis. (b) Main peak acceptable accuracy synthesis.

c) CCVT model for real-time simulation

A very accurate CCVT model can be obtained by combining the PT model described above with corresponding models for the tuning reactor, ferroresonance suppression circuit and the C's of the capacitive divider, in a similar manner to that suggested in [8]. In the context of a real-time simulator like RTNS [1], however, even though the CCVT model can be coded in a DSP board, execution speed is still important. If the real-time simulator is to be used, for example, for relay testing and solution steps of about 50 μs are acceped, the maximum accurate bandwidth of the simulation is around 2 to 4 kHz due to the distortion of the integration rule.

Our experience in this case is that for transients up to a few kilohertz, it is sufficient to approximate only the first resonant region of the short-circuit response of the magnetic device (Fig. 7). A very reasonable approximation of this region can be achieved with a simple *RLC* combination: R_0, L_0, C_1 (Fig. 8b). In this minimal approximation, R_0 and L_0 can be taken as the 60 Hz values, while C_1 is calculated to match the first resonant peak.

We are currently in the process of implementing this model in our real-time simulator RTNS. It should be emphasized that the proposed approach leads to a general two-port model for the CCVT device and, therefore, it can be used for any value of burden connected to the output port. Also, the clear identification in the model of the magnetization branch of the potential transformer permits the addition of as much detail as needed (depending on the PT design) for the representation of saturation and hysteresis phenomena.

It should also be mentioned that the accuracy that can be obtained even with a single *RLC* block in the proposed model for magnetic devices is due, in large part, to the topological separation in the model of the constant-valued stray capacitances from the frequency dependent short circuit branch. This separation cannot be easily achieved with *black box* models based on measured "open-circuit" terminal responses (e.g., the $[Y(\omega)]$ transformer admittance description).

4. Conclusions

This paper has presented models for current transformers and coupling capacitor voltage transformers suitable for real-time transients simulation. The *CT* model represents saturation using a piecewise linear representation. Algorithmic efficiency is achieved by eliminating unnecessary internal nodes in the model. The paper also reports on recent work on the modelling of frequency responses of transformer devices. The transformer model developed achieves the correct frequency response by a clear topological separation of the parasitical capacitances from the leakage and copper losses of the windings. The capacitances are constant and the frequency dependent effects are concentrated on the short-circuit impedance branch. A simplified version of this general model, consisting of a single *RLC* branch, is sufficiently accurate for real-time simulations with time steps in the order of 50 μs.

5. References

[1] J.R.Marti and L.R.Linares, "*Real-Time EMTP-based transients simulation*," IEEE Trans. on Power Systems, Vol. 9, No. 3, August 1994, pp. 1309-1317.

[2] H.W.Dommel, *EMTP Theory Book* (book), Microtran Power Systems Analysis Corporation, Vancouver, Canada, May 1992.

[3] H.W.Dommel, *Case Studies for Electromagnetic Transients* (book), Microtran Power System Analysis

Corporation, Vancouver, Canada, September 1993.

[4] M.Kezunovic, C.W.Fromen, and F.Philips, "*Experimental Evaluation of EMTP-based Current Transformer Models for Protective Relay Transient Study,*" IEEE Trans. on Power Delivery, Vol. 9, No 1, January 1994, pp. 405-413.

[5] M.Kezunovic et al., C.W.Fromen et al., and S.L.Nilsson, "*Digital Models of Coupling Capacitor Voltage Transformers for Protective Relay Transient Studies*", IEEE Trans. on Power Delivery, Vol. 7, No. 4, October 1992, pp. 1927-1935.

[6] Lj.Kojovic, M.Kezunovic et al., and C.W.Fromen et al., "*A New Method for the CCVT Performance Analysis Using Field Measurements, Signal Processing and EMTP Modeling*", IEEE Trans. on Power Delivery, Vol. 9, No. 4, October 1994, pp. 1907-1915.

[7] S.Chimklai and J.R.Marti, "*Simplified Three-Phase Transformer Model for Electromagnetic Transient Studies*". To be published in IEEE Trans. on Power Delivery. Paper 94SM410-1 PWRD, July 1994, 8 pages.

[8] J.R.Lucas, P.G.McLaren, W.W.L.Keerthipala, and R.P.Jayasinghe, "*Improved Simulation Models for Current and Voltage Transformers in Relay Studies,*" Trans. on Power Delivery, Vol. 7, No. 1, January 1992., pp. 152-159.

[9] G.R.Slemon and A.Stranghen, *Electric Machines* (book), Addison-Wesley, pp. 139-141, 1980.

5. BIOGRAPHIES

Jose R. Marti was born in Lerida, Spain in 1948. He received the degree of Electrical Engineer from Central University of Venezuela in 1971, the degree of M.E.E.P. from Rensselaer Polytechnic Institute in 1974 and the Ph.D degree from the University of British Columbia in 1981. In Venezuela, he worked for industry and taught at Central University of Venezuela. He has been a professor with the University of British Columbia, Canada, since 1988, where he has been working in the development of models and solution techniques for the transient analysis program EMTP. He is a registered professional engineer in British Columbia, Canada.

Luis R. Linares was born in Venezuela in 1957. He received the degree of Electrical Engineer from Central University of Venezuela in 1981, the degree of M.A.Sc from the University of British Columbia in 1993, and is currently working toward the Ph.D. degree at the University of British Columbia, Vancouver, Canada. Mr. Linares has worked for industry both as an electrical engineer and as a solftware engineer. He also taught at Central University of Venezuela.

Hermann W. Dommel was born in Germany in 1933. He received the Dipl.-Ing. and Dr.-Ing. degrees in electrical engineering from the Technical University, Munich, Germany in 1959 and 1962, respectively. From 1959 to 1966 he was with the Technical University Munich, and from 1966 to 1973 with Bonneville Power Administration, Potland, Oregon. Since July 1973 he has been with the University of British Columbia in Vancouver, Canada. Dr. Dommel is a Fellow of IEEE and a registered professional engineer in British Columbia, Canada.